8B.1 Observations from VORTEX2: The pretornadic phase of the Goshen County, Wyoming, supercell

PAUL MARKOWSKI,* YVETTE RICHARDSON, JIM MARQUIS

Department of Meteorology, Pennsylvania State University, University Park, PA

JOSHUA WURMAN, KAREN KOSIBA, PAUL ROBINSON

Center for Severe Weather Research, Boulder, Colorado

ROBERT DAVIES-JONES

Norfolk, England

ERIK RASMUSSEN

Rasmussen Systems, Mesa, Colorado

DAVID DOWELL

NOAA Earth System Research Laboratory, Boulder, Colorado

1. Introduction

The 5 June 2009 tornadic supercell in Goshen County, Wyoming, is among the best-sampled storms intercepted by the Second Verification of the Origins of Rotation in Tornadoes Experiment (VORTEX2). The storm developed from a cluster of cells that was initiated north of Cheyenne, Wyoming, shortly after 2000 UTC, in a region of south-southeasterly upslope flow at the surface. The convection formed beneath seasonably strong west-southwesterly winds in the mid- to upper-troposphere associated with an approaching upper-level trough. The vertical wind profile was characterized by significant shear (e.g., the 0–3 km storm-relative helicity and magnitude of the 0–6 km vector wind difference were $\sim$170 m^2 s^{-2} and $\sim$30 m s^{-1}, respectively, and the convective available potential energy inferred from nearby soundings was roughly 2000–3000 J kg^{-1}, depending on which parcel's ascent was analyzed on a thermodynamic diagram.

The storm began exhibiting supercellular characteristics (e.g., an echo appendage on the right rear flank at low levels, cyclonic azimuthal wind shear in the radial velocity data at midlevels) by shortly after 2100 UTC, which was approximately the time that the VORTEX2 assets made the decision to target the storm. A prominent hook echo was evident in reflectivity data by 2130 UTC. Rotation rapidly increased after 2142 UTC (a "coiled" hook echo was apparent by 2148 UTC), and increased to tornado strength by 2152 UTC. The tornado, which tracked through the center of the region of dual-Doppler radar coverage, intensified in the 2152–2202 UTC period, reached a maximum intensity of EF2 per mobile radar observations (Wurman et al. 2011), and eventually dissipated at 2230 UTC near LaGrange, Wyoming.

Our presentation is one of several on the Goshen County storm. The pretornadic phase of the storm (2100–2148 UTC) is treated in the present submission. Other presentations in the same session cover the genesis and intensification of the tornado (2248–2202 UTC; Kosiba et al. 2011), the time during which a relatively steady tornado was observed (2202–2212 UTC; Wurman et al. 2011), and ensemble Kalman filter (EnKF) analyses of the storm (Marquis et al. 2011).

*Corresponding author address: Dr. Paul Markowski, Department of Meteorology, Pennsylvania State University, 503 Walker Building, University Park, PA 16802; *e-mail*: pmarkowski@psu.edu.

2. Summary of findings

A much lengthier analysis of the pretornadic phase of the Goshen County storm is nearing submission for formal publication in the peer-reviewed literature (available from the lead author upon request). What follows below represents a greatly abridged summary of the evolution of the storm during the period leading up to tornadogenesis. Additional details will be presented during the oral presentation.

At the time that dual-Doppler data collection began (2130 UTC), the regions of significant midlevel and low-level vertical vorticity (10^{-2} s^{-1}) are separated, per isosurface analyses, with the low-level mesocyclone located along the gust front and the midlevel mesocyclone leading the low-level mesocyclone by several kilometers (Fig. 1a). The vortex lines associated with the midlevel mesocyclone originate in the environment to the south. In contrast, the vortex lines lines associated with the low-level mesocyclone form arches that joined the cyclonic vorticity region with a mesoanticyclone in the outflow trailing the hook echo. The configuration of these vortex lines suggests that they were generated or strongly modified by baroclinity (Straka et al. 2007; Markowski et al. 2008).

The region of significant cyclonic vertical vorticity at low levels gradually grows upward and into the region of significant midlevel vertical vorticity, resulting in a single column of vertical vorticity that spanned the depth of the radar observations by 2140 UTC (Fig. 1b). A descending reflectivity core (DRC; Rasmussen et al. 2006; Kennedy et al. 2007a,b; Byko et al. 2009) then develops at midlevels to the rear of the updraft, and its descent to the surface is accompanied by the rapid intensification of cyclonic vorticity at low- and midlevels (Fig. 1c,d). Anticyclonic vorticity also intensifies, though to a far lesser degree than the amplification of cyclonic vorticity.

By 2148 UTC, the gust fronts acquire a familiar occluded structure, with the rear-flank gust front wrapping around the circulation center. Strong rotation ($\zeta > 0.02$ s^{-1}) extends from the lowest levels scanned by the radars to midlevels, though two distinct vorticity maxima still can be identified at midlevels (one is associated with environmental vortex lines that have been tilted to form the original midlevel mesocyclone, the other is associated with the upward development of the vortex line arches that originate in the outflow at low levels). The tornado that develops in the ensuing minutes is associated with this deep

column of strong rotation.

We have high confidence in the following conclusions:

1. The θ_v observed at the surface, within the outflow, a short distance ($\sim$3 km) upstream of the location of ζ_{max}, was no more than 3 K colder than the warmest θ_v readings in the inflow of the storm. Larger θ_v deficits (up to 6 K) were observed to the rear of the hook echo and within the heavy precipitation to the north of the updraft.

2. The θ_e field observed at the surface had a structure similar to the θ_v field, i.e., θ_e decreased within the outflow to the west and northwest. The regions of lowest θ_e at the surface corresponded to the regions where air had descended from the highest altitudes.

3. Forward trajectories originating in the intensifying low-level mesocyclone rose rapidly in 2142–2148 UTC period (in contrast to the trajectories originating in some nontornadic low-level mesocyclones that have been documented recently; Markowski et al. 2011). The upward accelerations imply that the upward-directed vertical perturbation pressure gradient force (VPPGF) exceeded the negative buoyancy.

4. The rapid increase in low-level circulation (about a fixed ring encircling ζ_{max}) and vertical vorticity in the 2142–2148 UTC period was triggered by a DRC. Though the vast majority of the circulation about material circuits converging upon the low-level mesocyclone appears to have been acquired in the forward-flank baroclinic zone (see conclusion no. 7), the DRC had an important modulating influence on the circulation of the material circuits. A circuit that arrived at the location of ζ_{max} prior to the DRC's arrival at low levels lost some of its previously acquired circulation during its final few minutes of approach to the location of ζ_{max}. In contrast, a circuit that approached the location of ζ_{max} after the DRC had arrived at low levels—a significant segment of this circuit passed through the DRC—did not experience the same adversity.

5. The enhanced reflectivity of the DRC was not the result of heavy rain, given that the DRC was practically transparent visually.

6. The DRC was associated with a new updraft pulse that developed on the right (south) flank of the storm and subsequently grew into the main updraft.

The following conclusions are more tentative:

7. The environmental vorticity did not contribute significantly to the circulation of the material circuits that converged upon the low-level mesocyclone. Most of the circulation was acquired in the forward-flank region, similar to the evolution in the simulation analyzed by Rotunno and Klemp (1985), and Bjerknes' theorem implies that baroclinity played a major role. (This finding depends on the credibility of the steady-state assumed in the 2132–2142 UTC period in order to extend the trajectory calculations beyond the start time of dual-Doppler scanning at low levels.)

8. The negative buoyancy observed in the forward-flank along the path of the circuits was too small to solely account for the rapid rate of circulation growth. (Although this finding must be considered tentative for the same reason given in no. 7, we are exploring the possibility that surface drag might have contributed to the low-level mesocyclone's circulation.)

9. Vertical vorticity grew along descending trajectories, as in the Davies-Jones and Brooks (1993) conceptual model. (We could not evaluate trends in the vorticity vector along backward trajectories originating within a kilometer of the location of ζ_{max} because these trajectories dropped below the radar data horizon.)

One of the goals of our ongoing research is to determine the roles played by environmental (barotropic) vorticity and storm-generated (baroclinic) vorticity. Our analysis strongly suggests that storm-generated vorticity was the dominant contributor to the circulation of the low-level mesocyclone. So what is the role of environmental vorticity? Our material circuit analyses show that the midlevel mesocyclone's circulation was derived from environmental vorticity, which is consistent with the vortex line analysis and long-standing theory (e.g., Rotunno 1981; Davies-Jones 1984). The fact that midlevel mesocyclone strength is only a mediocre predictor of tornadogenesis (Wakimoto et al. 2004; Trapp et al. 2005) would, on one hand, seem to imply that environmental vorticity is not all that important. On the other hand, the magnitude of the environmental vorticity, particularly in the lowest 500–1000 m, is used somewhat skillfully to discriminate between tornadic and nontornadic supercell environments (e.g., Craven and Brooks 2004). The latter observation suggests that environmental vorticity is relevant, but the former observation suggests that the role of environmental vorticity might be *indirect*, i.e., not simply tied to the strength of the midlevel mesocyclone that develops. Is large environmental vorticity important because it is associated with large environmental wind shear, with the strength of the upward-directed VPPGF at low levels (it must be strong enough to offset the negative buoyancy of the circulation-bearing outflow air) increasing as the low-level environmental shear increases? This was shown to be an important effect in the idealized numerical simulations of Markowski et al. (2010).

Acknowledgments. We are grateful for the support of VORTEX2 by the National Science Foundation (NSF) and National Oceanic and Atmospheric Administration (NOAA). We also thank the countless number of VORTEX2 PIs, students, and other participants, without which the project would not have been possible. Jim LaDue, Nolan Atkins, Roger Wakimoto, and the University of Oklahoma and Lyndon State University-NCAR photogrammetry groups provided photographs and video.

REFERENCES

Byko, Z., P. Markowski, Y. Richardson, J. Wurman, and E. Adlerman, 2009: Descending reflectivity cores in supercell thunderstorms observed by mobile radars and in a high-resolution numerical simulation. *Wea. Forecasting*, **24**, 155–186.

Craven, J. P., and H. E. Brooks, 2004: Baseline climatology of sounding derived parameters associated with deep, moist convection. *Nat. Wea. Digest*, **28**, 13–24.

Davies-Jones, R. P., 1984: Streamwise vorticity: The origin of updraft rotation in supercell storms. *J. Atmos. Sci.*, **41**, 2991–3006.

Davies-Jones, R. P., and H.E. Brooks, 1993: Mesocyclogenesis from a theoretical perspective. *The Tornado: Its Structure, Dynamics, Prediction, and Hazards, Geophys. Monogr.*, No. 79, Amer. Geophys. Union, 105–114.

Kennedy, A. D., J. M. Straka, and E. N. Rasmussen, 2007a: A statistical study of the association of DRCs with supercells and tornadoes. *Wea. Forecasting*, **22**, 1192–1199.

Kennedy, A. D., J. M. Straka, and E. N. Rasmussen, 2007b: A visual observation of the 6 June 2005 descending reflectivity core. *E. J. Severe Storms Met.*, **2**(6).

Kosiba, K., J. Wurman, Y. Richardson, P. Markowski, and P. Robinson, 2011: The genesis of the Goshen County, Wyoming, tornado (5 June 2009). Preprints, *35th Radar Conference*, Pittsburgh, PA, Amer. Meteor. Soc.

Markowski, P. M., J. M. Straka, E. N. Rasmussen, R. P. Davies-Jones, Y. Richardson, and J. Trapp, 2008: Vortex lines within low-level mesocyclones obtained from pseudo-dual-Doppler radar observations. *Mon. Wea. Rev.*, **136**, 3513–3535.

Markowski, P., M. Majcen, and Y. Richardson, 2010: Near-surface vortexgenesis in idealized three-dimensional numerical simulations involving a heat source and a heat sink in a vertically sheared environment. Preprints, *25th Conf. on Severe Local Storms*, Denver, Colorado, Amer. Meteor. Soc.

Markowski, P. M., M. Majcen, Y. P. Richardson, J. Marquis, and J. Wurman, 2011: Characteristics of the wind field in three nontornadic low-level mesocyclones observed by the Doppler On Wheels radars. *E. Journal of Severe Storms Meteor.*, **6** (3), 1–48.

Marquis, J., Y. Richardson, P. Markowski, D. Dowell, J. M. Wurman, K. Kosiba, and P. Robinson, 2011: Preliminary analysis of the Goshen County tornadic supercell on 5 June 2009 during VORTEX2 using EnKF analyses of mobile radar and mesonet data. Preprints, *35th Radar Conference*, Pittsburgh, PA, Amer. Meteor. Soc.

Rasmussen, E. N., J. M. Straka, M. S. Gilmore, and R. Davies-Jones, 2006: A preliminary survey of rear-flank descending reflectivity cores in supercell storms. *Wea. Forecasting*, **21**, 923–938.

Rotunno, R., 1981: On the evolution of thunderstorm rotation. *Mon. Wea. Rev.*, **109**, 577–586.

Rotunno, R., and J. B. Klemp, 1985: On the rotation and propagation of simulated supercell thunderstorms. *J. Atmos. Sci.*, **42**, 271–292.

Straka, J. M., E. N. Rasmussen, R. P. Davies-Jones, and P. M. Markowski, 2007: An observational and idealized numerical examination of low-level counter-rotating vortices toward the rear flank of supercells. *E. Journal of Severe Storms Meteor.*, **2(8)**, 1–22.

Trapp, R. J., G. J. Stumpf, and K. L. Manross, 2005: A reassessment of the percentage of tornadic mesocyclones. *Wea. Forecasting*, **20**, 680–687.

Wakimoto, R. M., H. Cai, and H. V. Murphey, 2004: The Superior, Nebraska, supercell during BAMEX. *Bull. Amer. Meteor. Soc.*, **85**, 1095–1106.

Wurman, J., K. Kosiba, Y. Richardson, P. Markowski, and P. Robinson, 2011: The intensification of the Goshen County, Wyoming, tornado (5 June 2009). Preprints, *35th Radar Conference*, Pittsburgh, PA, Amer. Meteor. Soc.

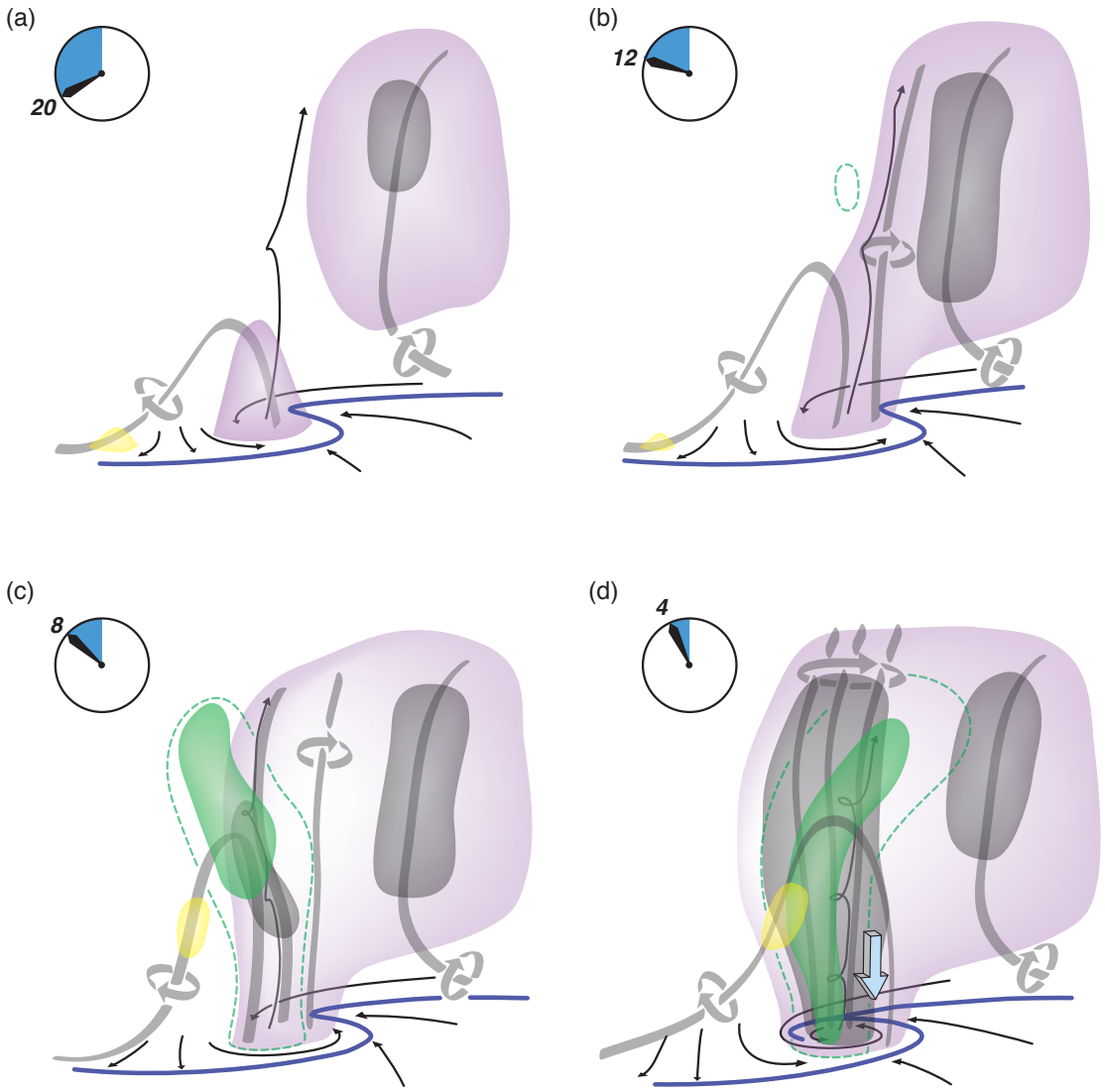

FIG. 1. Schematic summarizing the evolution of the Goshen County storm during its pretornadic phase: (a) 2130–2135 UTC (∼20 min prior to tornadogenesis, as indicated by the hand on the clock), (b) 2135–2140 UTC (∼12 min prior to tornadogenesis), (c) 2142–2144 (∼8 min prior to tornadogenesis), and (d) 2146–2148 (∼4 min prior to tornadogenesis). The yellow and purple isosurfaces indicate regions of significant anticyclonic and cyclonic vertical vorticity ($\pm 0.01\ s^{-1}$), and the dark gray isosurfaces enclose regions of even larger cyclonic vertical vorticity ($0.02\ s^{-1}$). The DRC is indicated by the green isosurface. Surface gust fronts are analyzed using blue lines. Streamlines are drawn using black arrows. Vortex lines are gray (the sense of rotation is indicated by the gray arrows). In (d), the broad downward-pointing arrow indicates an occlusion downdraft. North is into the page.